Mechanical Interactions in All-Carbon Peapods

Manuel Melle-Franco,† Hans Kuzmany,‡ and Francesco Zerbetto*,†

Dipartimento di Chimica "G. Ciamician", Università di Bologna, V. F. Selmi 2, 40126 Bologna, Italy, and Institut für Materialphysik, Universität Wien, Strudlhofgasse 4, A-1090 Wien, Austria

Received: December 9, 2002; In Final Form: May 12, 2003

Structures and energetics of several types of all-carbon peapods made by C_{60}s encapsulated inside single-wall carbon nanotubes are calculated. The interactions between the tubes and the molecules determine a minimal diameter for exothermic encapsulation of 11.74 Å and a radial deformation of the C_{60} cage that is a linear function of the tube diameter. Many relative orientations of the "peas" have similar energies and can be thermally equilibrated, although preferential ways of interaction between fullerenes do exist. In particular, for a triplet of embedded fullerenes, the lowest energy arrangement is characterized by a facing describable as pentagon-hexagon-pentagon. The activation energy for the translation of isolated C_{60} molecules inside the tubes is very low and an isolated C_{60} can diffuse freely inside the pod: The major factor controlling the dynamics of molecular transport in the peapods is therefore the $C_{60}-C_{60}$ interaction.

Introduction

Nanopeapods, that is, fullerene molecules encapsulated inside a single-wall carbon nanotube, SWCNT, are emerging as a class of nanoscale materials with tunable properties.[1] In these all-carbon systems, C_{60} modifies the local electronic structure of the nanotube, NT, mixing its orbitals with the nanotube's electronic band,[1] while the SWCNT vessels modify the fullerene chemical reactivity, altering the conduction properties of the system.[2]

The elucidation of the structural and dynamical properties of all-carbon peapods is one of the crucial steps toward their practical exploitation. Molecular modeling can assist this process and was able, for instance, to show that the binding energy of a fullerene inside a (10,10) metallic nanotube is slightly more than 75 kcal mol^{-1} (3.26 eV).[3] The (n,m) notation,[4,5] of which (10,10) is an example, defines the unit cell of the 2D graphite lattice rolled up to form the tube: $m = 0$ identifies zigzag tubes, while $n = m$ identifies armchair, metallic, nonchiral tubes. To date, the (10,10) tubes have been the subject of a large number of theoretical studies, although the experimental relative abundance of the various (n,m) forms is still open to debate.[6] The 75 kcal mol^{-1} C_{60}-tube binding energy calculated by Girifalco et al.[3] is in contrast with a value of 11.8 kcal mol^{-1} (0.51 eV) given elsewhere.[7] The difference likely arises from the different nature of the calculations. The larger value was obtained with an ad hoc potential developed and tested for carbon; the smaller value is the result of local density approximation, LDA, calculations, which do not include dispersion forces. An interesting result obtained by the interpolation of the LDA calculations for three different peapods is that the smallest SWCNT diameter able to encapsulate exothermically C_{60} is 12.8 Å.

As far as we are aware, calculations reported to date on all-carbon peapods have, in the great majority, only considered tubes with $n = m$. Here, we investigate computationally a number of peapods made with general (n,m) tubes, which are also characterized by different filling ratios. The scope is to confirm and generalize the results obtained previously, to determine the binding energy of C_{60} inside a generic SWCNT without the constrain of $m = n$, to calculate the deformation energy of the nanotubes and the related aspect ratio of C_{60} inside them, to discern what are the preferential orientations of the fullerenes with respect to each other inside the tube, and to assess what are the major factors governing the dynamics of peapods.

Computational Background

To describe the peapods, we employ Brenner potential.[8] Some tuning was required for an accurate description of the intermolecular, i.e. $NT-C_{60}$, interactions that were described by the relevant part of the MM3 potential that was parametrized on a variety of organics and graphite.[9] MM3 was successful in the description of the subtle effects that lead to C_{60} spinning in clusters.[10]

To test the present combined model we reproduced the so-called AB structure of graphite, which gave an interlayer distance of 3.379 Å (experimentally 3.354 Å[4]) and CC distance of 1.417 Å (experimentally 1.421 Å[4]). We also obtained 16.6 Å for the minimum intertube distance in (10,10) clusters (experimentally, 16.76 ± 0.05 Å[11]). Finally, as a further test for validating the model, we calculated the packing energy of C_{60} crystals, which resulted in 1.74 eV, comparable with the reported value of 1.6 eV.[4] The present approach was recently used to model the effect of permanent twisting of SWCNT.[12] The cutoff for the interatomic potential was set to 10 Å, after checking that the procedure gave accurate results for graphite. Periodic boundary conditions were used axially. When partial filling ratios with more than one C_{60} per tube were simulated, the free region inside the nanotube was set to at least 10 Å on each side of the encapsulated molecule(s).

The large number of minima present in some of the systems induced us to develop a procedure to explore systematically the configurational space. This procedure was divided in two parts: in the first part a consecutive series of minimizations of

* Corresponding author: phone + 39 051 209 94 73; fax + 39 051 209 94 56; e-mail gatto@ciam.unibo.it.
† Università di Bologna.
‡ Universität Wien.

10.1021/jp027658e CCC: $25.00
Published on Web 06/26/2003

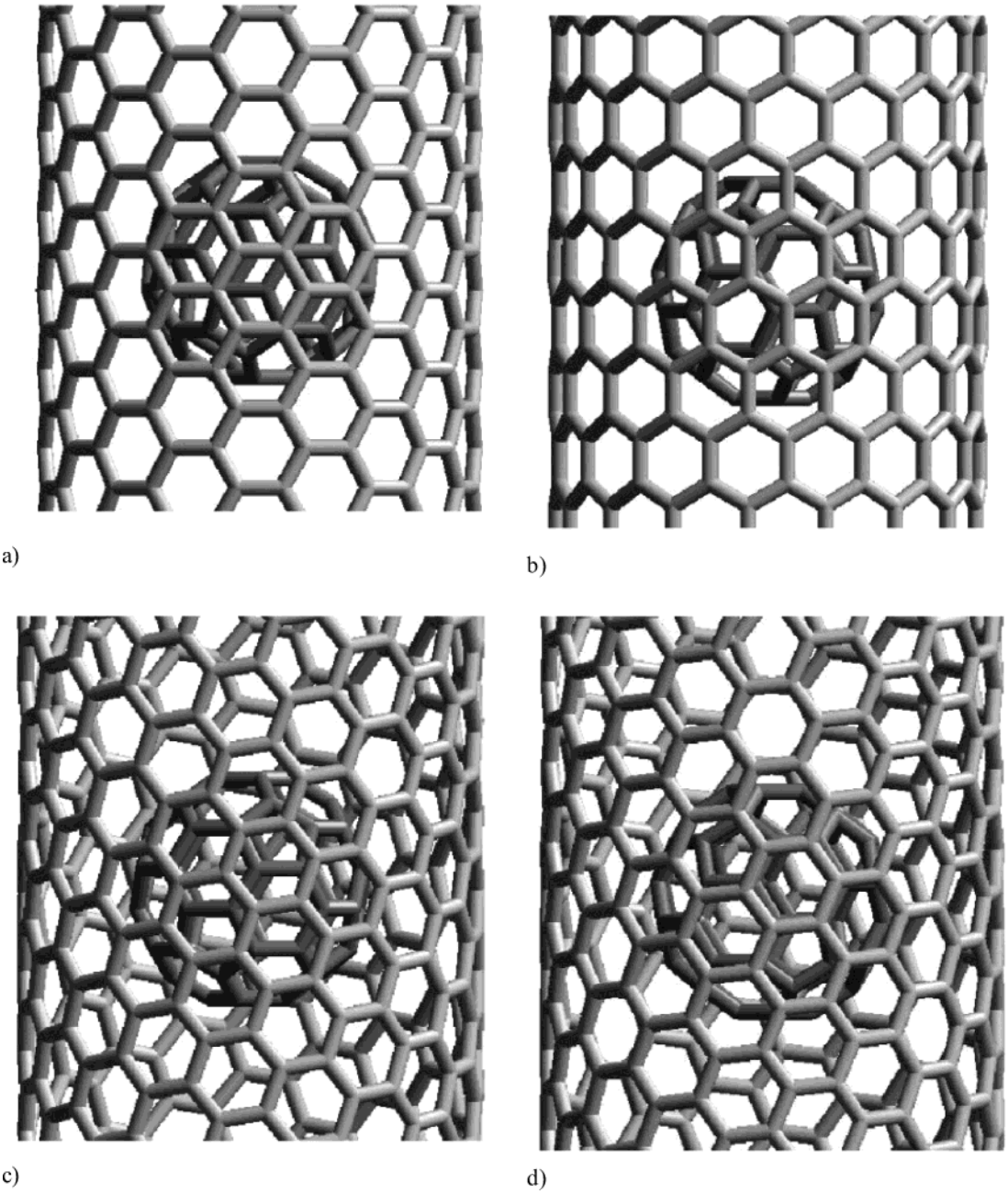

Figure 1. Some of the peapods investigated in this work: (a) (10,10) peapod; (b) (17,0) peapod; (c) (13,7) peapod; (d) (12,8) peapod.

rigid C_{60} molecules followed by random reorientation was performed an arbitrary number of times (typically 200, but values up to 1000 were tried with similar results). In the second part all the different minima were further minimized without constraints, and their nature was confirmed by vibrational analysis.

Results and Discussion

The majority of the discussion of the results obtained in the investigation of the peapods will be centered on the simulations performed with (10,10), (17,0), (13,7), and (12,8) pods, but calculations on peapods with (8,8), (15,0), (9,9), (16,0), (17,0), (18,0), (19,0), and (11,11) NT are also reported. The first set of peapods (see Figure 1) was chosen because the diameters of the NT range from 13.3 to 13.8 Å, i.e., the best region to encapsulate C_{60}, and because they span a number of situations: (10,10), the most widely used SWCNT in the simulations (probably for the simplicity of its structure), is an armchair, cis-type, nonchiral structure that is metallic and belongs to D_{10h} point group; (17,0) is a zigzag, trans-type, nonchiral structure that is semiconducting and belongs to D_{17d} point group; (13,7) is chiral, metallic, and belongs to C_1 point group; and (12,8) is chiral, semiconducting, and belongs to C_4 point group.

A relevant feature to consider when performing calculations with periodic boundary conditions is the size of the unit cell, which differs greatly for the four fully packed peapods. The unit cell for a single C_{60} is 9.9 ± 0.1 Å and may, or more likely may not, be commensurate with the NT cell. In general, NTs must have more than one C_{60} per unit cell: (10,10) is the only NT that requires a supracell of four unit cells to contain a single C_{60}. In the other three cases, commensurability between the NT and C_{60} cells is reached only by having several C_{60}s per cell [3 for (17,0), 5 for (13,7), and 13 for (12,8)]. Therefore, depending on the system, the length of peapod treated explicitly changes and ranges from 9.84 Å for (10,10) to 129.99 Å for (12,8).

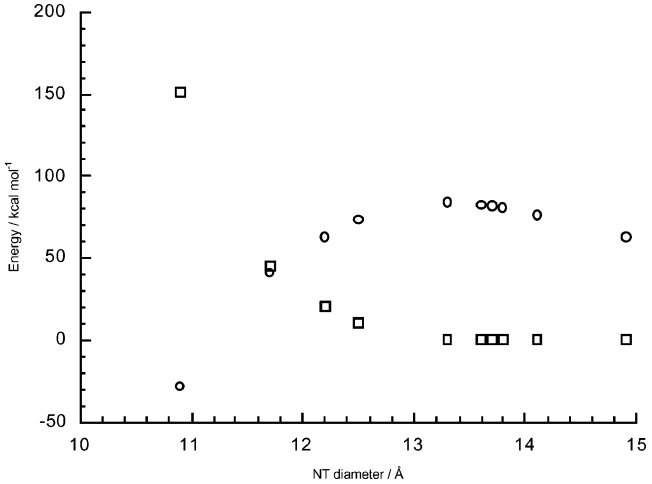

Figure 2. Calculated binding (○) and distortion (□) energies vs SWCNT diameter. Notice the different, but standard, convention adopted for the signs of the two type of energies.

Encapsulation of C_{60} in a tube produces two different effects: (a) it gives an energy of interaction between the molecule and the tube, which may be binding or not binding, and (b) the nanotube and the encapsulated molecules deform, which entails an energy penalty. Figure 2 presents plots of (a) the purely binding intermolecular energy, and (b) the deformation energy of guest and host vs the tube diameter. The plots are for a single fullerene encapsulated inside different (*m*,*n*) nanotubes. They cover (i) the region where insertion of C_{60} is energetically costly (because of the narrowness of the NT), (ii) the diameters where the fullerene is snugly accommodated inside the tube, and (iii) the region where the nanotube internal cavity is large compared to the encapsulated C_{60}: in this case, the fullerene sits closer to a part of the wall of the NT than to the part diametrically opposite. Interpolation of the data of Figure 2 gives 11.74 Å as the minimal diameter for exothermic encapsulation.

The values for adsorption on the external wall of the tube are very similar for all the tubes considered here and correspond to only a fraction of the energy value for the encapsulation. In the same notation used above, the binding (deformation) energies are 82.27 (0.38), 83.42 (0.82), 80.55 (0.30), and 81.64 (0.32) kcal mol^{-1} for (10, 10), (17,0), (13,7) and (12,8), while for adsorption on a graphite crystal surface we calculate 22.96 (0.91) kcal mol^{-1}.

In the "tight" fitting region, the aspect ratio of C_{60} becomes of interest. The presence of a host with a narrow diameter deforms the fullerenic cage and makes it ellipsoidal with one long and two short diameters, i.e., the molecule becomes prolate. Figure 3 shows the variation of the diameters with respect to that of free C_{60}. The trends are linear. Notice that for (8,8), two different types of deformations, i.e., minima, were located and are reported. Consistently, for all the peapods, the elongation of the C_{60} radius along the axial direction of the nanotube is smaller than the shortening of the radii that point toward the tube wall.

When C_{60} inside a NT becomes prolate, the host can exhibit a corresponding swelling. Indeed, Figure 4 shows what happens in the rather extreme case of (8,8), where the NT radius increases by 0.4 Å. Similarly, in (9,9) and in (15,0) the NT radius elongation is 0.2 Å and this variation tapers off to 0.1 Å for (16,0). The bulging should be visible experimentally. The opposite effect of C_{60} becoming oblate with the NT walls

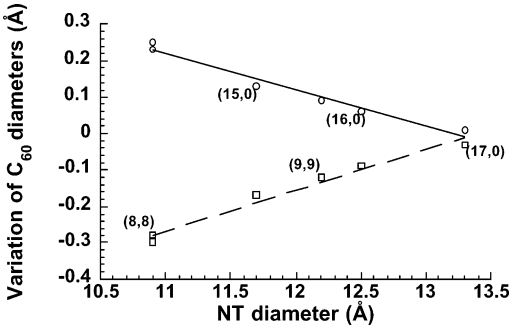

Figure 3. Variation of the two independent fullerene diameters as a function of the SWCNT diamter.

reaching inside is hardly apparent in the calculations, with the NT radius reduced by less than 0.05 Å in all cases examined here.

Apart from the interaction between a SWCNT and encapsulated C_{60}, a further aspect to consider is the $C_{60}-C_{60}$ interaction. This is modeled by considering clusters of three fullerenes inside each tube. Equivalent studies with larger and smaller clusters show that the energy of the different conformations is very similar regardless of the number of C_{60} molecules. This finding is easily explained since, due to the size of C_{60} and the effective range of intermolecular interactions, each C_{60} only interacts with its surrounding portion of the tube and its two nearby neighbors. During the simulations, it became immediately apparent that the molecules give rise to a large number of low-lying minima with similar energies. To investigate systematically the minima, a very large number of C_{60} rotational orientations were generated. They differ in the relative orientation of the molecules with respect to one another, that is, in the way the two pairs of fullerenes face each other. The four main structural motifs present in C_{60} are the pentagon, the hexagon, the pentagon−hexagon bond, and the hexagon−hexagon bond, and it is probably best to describe the interactions between C_{60}s in terms of their interacting hexagonal and pentagonal faces as they are observed looking down the tube. A simple labeling scheme uses P for pentagon and H for hexagon. Since in C_{60} the face opposite any other face has the same shape, three letters suffice to define the interactions in a triplet of fullerenes. They are PPP, PPH ≡ HPP, PHP, PHH ≡ HHP (not observed), HPH, and HHH. As a practical example, PPP means that the faces of the C_{60}s observed from the NT axis are mainly three pentagons. The most stable arrangements found in all the calculations are consistently PHP followed by PPP. It is interesting to notice that for the energies of the most stable PHP and PPP configurations there is a linear correlation between binding energy and face-to-face distance between the C_{60}s (see Figure 5). The existence of a varying distance between the facial orientations (see also Table 1) may result from small but finite dimerization effects, where the distance between two adjacent fullerenes is smaller than that between one of them and one of the next-neighbor pair.

The remaining facial arrangements also show some correlations but not as well defined as PHP and PPP (see Table 1 for the energies). Because of the small energy differences, the minima can be in thermal equilibrium at room temperature. Calculations on fully packed SWCNTs were also performed and in all representative cases they gave results very similar to those obtained for the corresponding cluster.

A common feature of all the conformations explored is the presence of very soft vibrational frequencies corresponding to rotational and translational motions of the encapsulated C_{60}

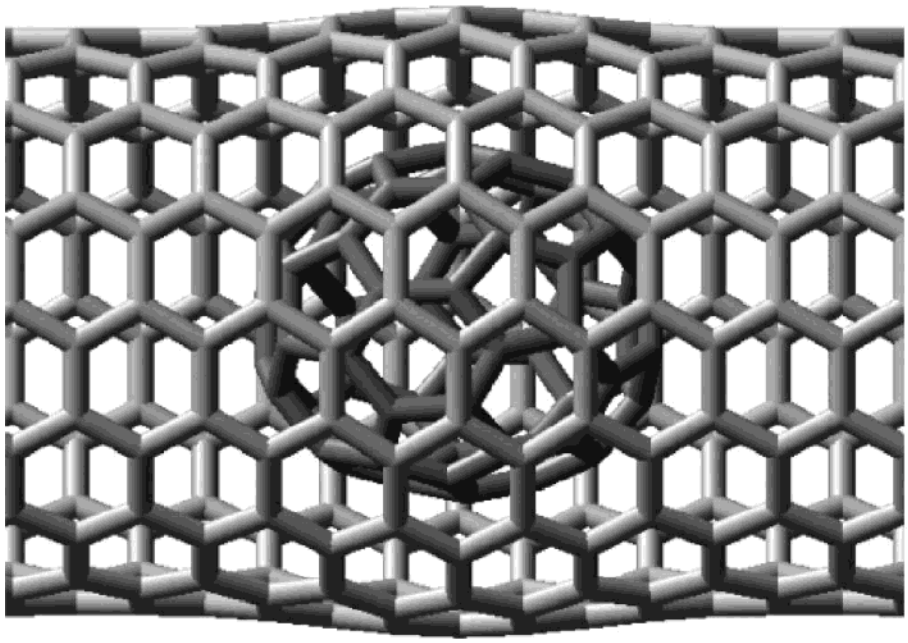

Figure 4. Swelling of the (8,8) NT due to the presence of C_{60}.

TABLE 1: Ranges of Center-to-Center Distances and Binding Energies of C_{60} Pairs Inside the Nanotubes[a]

	(10,10)		(17,0)		(13,7)		(12,8)	
NT	distance	energy	distance	energy	distance	energy	distance	energy
PHP	9.88−9.89	6.43−6.44	9.91	6.36	9.85−9.87	6.52−6.54	9.87−9.88	6.48−6.49
PPP	9.96−9.97	6.36−6.38	9.99	6.32	9.95	6.39	9.96	6.38−6.39
HHH	9.82−9.83	6.26	9.99	6.17	9.95	6.33−6.34	9.96	6.30
HPP	9.82−9.83	6.25	9.89	5.93	9.83	6.31	9.87−9.86	6.22−6.23
HPH	9.82−9.83	6.12−6.14	9.85	5.91	9.86	6.30	not found	not found

[a] Distances are given in angstroms; energies are given in kilocalories per mole.

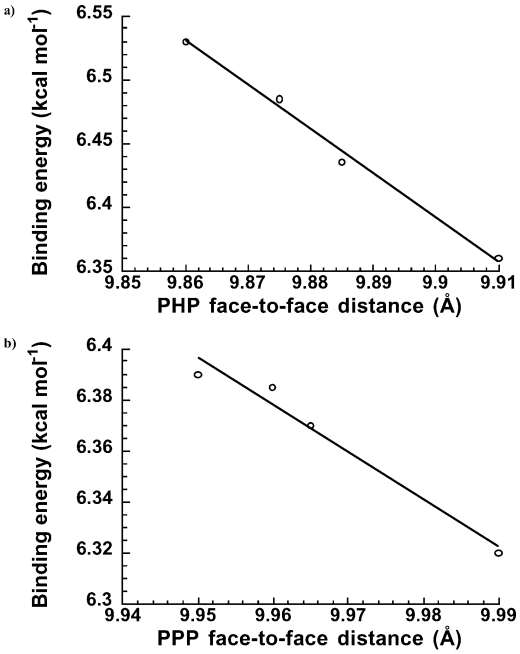

Figure 5. (a) Energy of interaction of a C_{60} pair inside different NTs for the most stable PHP arrangement, as a function of the optimized distance. (b) Energy of interaction of a C_{60} pair inside different NT for the second most stable PPP arrangement, as a function of the optimized distance.

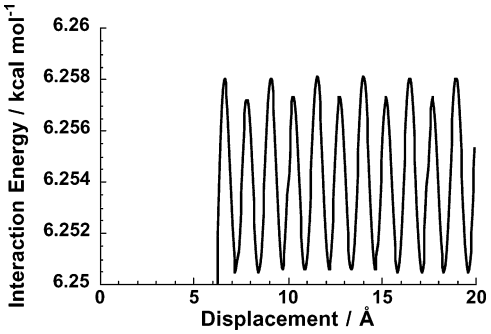

Figure 6. Oscillation of the energy for the displacement of a single C_{60} with perfect PPP facing inside a (10,10) SWCNT. Notice that at 0 Å the molecule is in van der Waals contact with other fullerenes. Detachment from the other C_{60}s requires overcoming an energy barrier (Table 1).

molecules (the values ranged from 0.2 to 2 cm^{-1}). Small energy barriers can accompany the low frequencies. Indeed, we found, depending on the SWCNT, that the translational energies ranged from 0.0025 to 0.011 kcal mol^{-1}. These astonishingly small values may seem a computational artifact until they are plotted to reveal a very well-defined periodicity that rules out the presence of numerical noise (see Figure 6). The low translation barrier also agrees with the plateaus found between multiple traversing paths of C_{60} inside a tube (see also Figure 6a of ref 13, which agrees with our finding) and with the idea that the motion inside the tube is mainly diffusional.[14] Notice that the energy barrier for C_{60} hopping along the tube is made up by this negligible contribution plus that due to the detachment of two neighboring fullerenes (Table 1).

The rotational motions were also considered. First, the rotation about the SWCNT axis gave a barrier of 0.01 kcal mol^{-1} and then a three-dimensional grid of 9×10^5 points was generated,

and we found that the highest energy point was 0.75 kcal mol^{-1} above the global minimum.

Conclusion

The guest−host interactions in all-carbon peapods lead to a number of relationships when they are correlated with the NT diameter. The smoothness of these correlations allows us to determine that the minimal diameter for exothermic encapsulation of C_{60} is 11.74 Å. A very large number of similar minima are found for the fullerene−fullerene interactions once they are embedded in a SWCNT. This indicates that the C_{60}s behave as real peas do inside a pod. Just as in peapods, the distance between the peas also can vary (up to 0.1 Å). The practical conclusion is that translational symmetry is very hard to attain in these systems. In view of the present calculations, several consequences can be expected in the spectra of C_{60} when used as a probe of the peapod properties: (a) the existence of disorder for the $C_{60}-C_{60}$ interactions and intermolecular distances can lead to line broadening; (b) the same disorder can effectively lower the symmetry and result in the disappearance of the typical symmetry properties of C_{60}; and (c) even when disorder is banished and long-range patterns of several C_{60} are formed, inside the unit cell of the peapod, the C_{60} distances can vary substantially, up to 0.1 Å, which, in turn, may produce (small) dimerization effects.

The calculations also find that there is a preferred orientation for the interaction of the fullerenes inside all the NT investigated here. If one looks down tubes with three guest molecules, such orientation can be described as the sequential facing of pentagon, hexagon, pentagon (in C_{60}, the face opposite any other face has the same shape). Since this motif appears regardless of the (*m*,*n*) structure of the NT, it is concluded that $C_{60}-C_{60}$, not C_{60}−NT, interactions determine the preferred rotational orientations of the encapsulated molecules.

Acknowledgment. This work was carried out with partial support from the European Union, Human Potential Network "FUNCARS" and Italian FIRB project.

References and Notes

(1) Hornbaker, D. J.; Kahng, S. J.; Misra, S.; Smith, B. W.; Johnson, A. T.; Mele, E. J.; Luzzi, D. E.; Yazdani, A. *Science* **2002**, *295*, 828−831.
(2) Pichler, T.; Kuzmany, H.; Kataura, H.; Achiba, Y. *Phys. Rev. Lett.* **2001**, *87*, 267401.
(3) Girifalco, L. A.; Hodak, M.; Lee, R. S. *Phys. Rev. B* **2000**, *62*, 13104−13110.
(4) Dresselhaus, M. S.; Dresselhaus, G.; Eklund, P. C. *Science of Fullerenes and Carbon Nanotubes*; Academic Press: San Diego, CA, 1996.
(5) Harris, P. J. F. *Carbon Nanotubes and Related Structures*; Cambridge University Press: Cambridge, U.K., 1999.
(6) Colomer, J.-F.; Henrard, L.; Lambin, Ph.; Van Tendeloo G. *Phys. Rev. B* **2001**, *64*, 125425-1−125425-7.
(7) Okada, S.; Saito, S.; Oshiyama, A. *Phys. Rev. Lett.* **2001**, *86*, 3835−3838.
(8) Brenner, D. W. *Phys. Rev. B* **1990**, *42*, 9458−9471.
(9) Allinger, N. L.; Yuh, Y. H.; Lii, J.-H. *J. Am. Chem. Soc.* **1989**, *23*, 8551−8566.
(10) Deleuze, M. S.; Zerbetto, F. *J. Am. Chem. Soc.* **1999**, *121*, 5281−5286.
(11) Yosida, Y. *J. Appl. Phys.* **2000**, *87*, 3338.
(12) Melle-Franco, M.; Prato, M.; Zerbetto, F. *J. Phys. Chem. A* **2002**, *106*, 4795−4797.
(13) Qian, D.; Liu, W. K.; Ruoff, R. S. *J. Phys. Chem. B* **2001**, *105*, 10753−10758.
(14) Berber, S.; Kwon, Y.-K.; Tomanek, D. *Phys. Rev. Lett.* **2002**, *88*, 185502.